SEM AND AFM MORPHOLOGICAL STUDY OF ZNO FILMS DEPOSITED ON ETCHED SILICON SUBSTRATES USING DC MAGNETRON SPUTTERING

B. Abdallah *, M. Alnezami, R. Hussin, W. Zetoune

Atomic Energy Commission, Department of Physics, PO Box 6091, Damascus, Syria
*Corresponding author, E-mail: pscientific27@aec.org.sy (B. Abdallah), phone: +963-11-2132580, Fax:+963-11-6112289

Received: 07-07-2022 Accepted: 29-03-2023
Published: 31-03-2023

ABSTRACT

In this work, ZnO films were deposited by Direct Current (DC) magnetron sputtering, on polished silicon substrate Si(100) (non-etched), etched for 1 min, 5 min, 10 min and 15 min. The etching of the substrate was carried out by means of dry plasma at different time and they compared with non-etched substrates. Etched silicon substrate effect on the structural and morphological properties of ZnO films was examined, and a new nanostructure can be obtained by the modification in morphology of ZnO film, and this will obviously useful for the electrical and gas sensitivity applications. AFM have been used to investigate the morphology and the roughness behaviors of ZnO films growth on etched and non-etched silicon substrates. SEM images for the Si(100) etched and non-etched effectuated with two modes (surface top view and cross section), the SEM was used too for ZnO film deposited on etched substrate (the etched time increase from 1 to 15 min) and non-etched Si substrates.

X-ray Photoelectron Spectroscopy (XPS) and X-ray Diffraction (XRD) techniques were employed to investigate the elements contents of the ZnO films and the crystallographic properties, respectively. In addition, the variation of water contact angle data (WCA) related to roughness of the ZnO films deposited on etched Si substrate at different times were studied.

Keyword: etching of Si substrate; ZnO film; DC magnetron; surface morphology.

ESTUDIO MORFOLÓGICO SEM Y AFM DE PELÍCULAS DE ZNO DEPOSITADAS SOBRE SUSTRATOS DE SILICIO GRABADOS UTILIZANDO SPUTTER CON MAGNETRÓN DC

RESUMEN

En este trabajo, las películas de ZnO se depositaron mediante pulverización catódica con magnetrón de corriente continua (DC), sobre sustrato de silicio pulido Si(100) (sin grabar), grabado durante 1 min, 5 min, 10 min y 15 min. El grabado del sustrato se realizó mediante plasma seco a diferentes tiempos y se compararon con sustratos no grabados. Se examinó el efecto del sustrato de silicio grabado en las propiedades estructurales y morfológicas de las películas de ZnO, y se puede obtener una nueva nanoestructura mediante la modificación de la morfología de la película de ZnO, y esto obviamente será útil para las aplicaciones de sensibilidad eléctrica y de gas. AFM se ha utilizado para investigar la morfología y los comportamientos de rugosidad del crecimiento de películas de ZnO en sustratos de silicio grabados y no grabados. Imágenes SEM para el Si(100) grabado y no grabado efectuado con dos modos (vista superior de la superficie y sección transversal), el SEM se usó también para la película de ZnO depositada en el sustrato grabado (el tiempo de grabado aumentó de 1 a 15 min) y Sustratos de Si no grabados. Se emplearon técnicas de espectroscopía de fotoelectrones de rayos X (XPS) y difracción de rayos X (XRD) para investigar el contenido de elementos de las películas de ZnO y las propiedades cristalográficas, respectivamente. Además, se estudió la variación de los datos del ángulo de contacto con el agua (WCA) relacionados con la rugosidad de las películas de ZnO depositadas sobre sustrato de Si grabado en diferentes tiempos.

Palabra claves: grabado de sustrato de Si; película de ZnO; magnetrón de DC; morfología de la superficie.

INTRODUCTION

The material nature and/or types (metal or semiconductors [1]) [2] [3; 4] and crystalline orientation of the substrate have distinguished the nucleation mechanism (up to down or down to up nanotubes) [5]. Also, the process of preparation influence on growth, dominated phases (cubic [6] or hexagonal [7]) of a thin film and its morphology as well as its physical properties. Deposition of polycrystalline, single crystalline [8] or amorphous thin films depends on the substrate as well as their chemistry (especially the interfaces) and growth conditions [9]. While for the same deposition method, the used parameters (such as the temperature, gas flux [10]), the stress and mismatch between the lattices of the substrate and of the deposited material play a vital role on the properties of the deposited film, especially near the contact interface [11]. Thickness of the films [3] can reduce the effect of the lattice mismatch between the substrate and the films [9]. RF (13.6 MHz radio frequency) is mainly used to deposit ZnO film. However, DC power is not frequently usable to deposited semiconductors film especially in magnetron sputtering because it is difficult to create the plasma than RF power [12] [13].

Recently a controlled ZnS as well as ZnO nanostructure appears to play a crucial role in optoelectronic devices performance [2] [14] and gas sensing response [15]. For example, Z-scan technique was employed to estimate the nonlinear optical absorption of the prepared semiconductors films[16] [17]. In general, one can adjust and manipulate the nanostructure [18; 19] to form nanosphere, core-shell, nanorod and nanowire by several means. Variation of the deposition parameters such as power, oxygen and pressure percentage in techniques using plasma like magnetron sputtering [10; 20] or by dry etching in plasma [21; 22] could use to achieve that. In magnetron sputtering, one can deposit films without annealing the substrates (room temperature), this is an advantage relative to the other processes especially for polymer substrate as well as substrate need a low temperature, these techniques much used to prepare semiconductor films, for example ZnO [23], SnO_2 [24], ZnS [7] and WO_3 [25] nanostructures of different morphologies as well as sol gel [26] ultrasonic spray pyrolysis [24; 27], pulsed laser deposition [4], plasma enhanced chemical vapor deposition (PECVD) [28] and thermal evaporation technique under vacuum [29; 30]; the last two techniques (PECVD and thermal evaporation) were necessary to heat the substrate more than 400^{o} C.

AFM and SEM were used to characterize ZnO film (deposited on etched Si) and compare that with non-etched substrate (which is considered as reference). The etched Si(100) substrate influence on the morphology (form and roughness) as well as the hydrophobicity (contact angle measurements) properties of the deposited film was studied. To our knowledge, no research work has been published relating to the study of the etching effect of the substrate by means of plasma PECDV on ZnO film prepared by DC sputtering.

EXPERIMENTAL SET-UP.

DC magnetron sputtering set up was utilized to deposit thin ZnO film on Si(100) substrate (etched and non-etched) using ZnO Target. The power was 100 w and deposition time was 7 min and the deposition rate was about 17 nm/min. The T chamber is home-made, it was manufactured from SS316, the residual pressure was 1x10^{-6} Torr and the working pressure was 7 mTorr at room temperature. The description of the vacuum system was cited in details in previous work [23]. PECDV dry plasma used to etch the Si(100) substrate at several times (etched times were 1min, 5 min, 10 min and 15 min) using SF_6 plasma [31] [32].

SEM (scanning electron microcopy TSCAN Vega\\XMU) and AFM (atomic force microscopy Park Scientific Instruments, AP-0100 model) have been used [33] to observe the surface modification on Si etched at different times as well as on ZnO film. Also, the superficial composition was performed by the XPS (X-ray Photoelectron Spectroscopy) analysis using SPECS UHV/XPS/AES spectrometer equipped XPS (with a monochromated AlKα X-ray radiation source at 1486.6 eV). The contact angle measurements were taken using the sessile drop technique (Data Physics Instrument GmbH

OCA 15 plus, SCA 20). The digitaldrop image was procedure by means of an image analysis system with an accuracy of ±0.1º[34].

RESULTS AND DISCUSSIONS

SEM AND AFM STUDY OF ETCHED Si(100)

Figure (1) shows SEM images of the surface of etched Si(100) for 1 min time, where (a) and (b) are at 50 k and 75 k magnifications, respectively. The silicon became porous and slightly rough, due to plasma SF_6 etched dry of PECVD. Similarly, Figures (1-c) and (1-d) show top view SEM images for etched Si(100) for 5 min at 50 k and 75 k magnifications, respectively. The silicon appeared more porous and the roughness increase considered as formed as the wires form, this result is in agreement with previous work where we used Ar+SF_6 plasma to etch the Si(100).

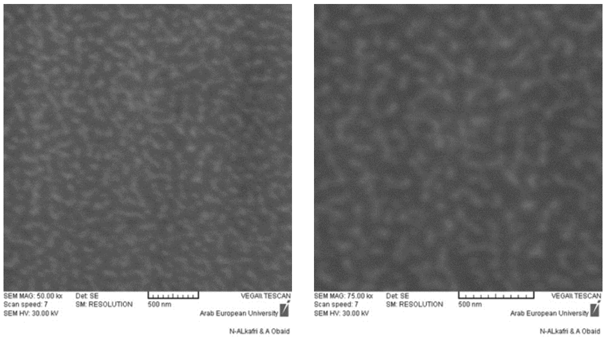

(a) Si etched for 1 min at 50 k Mag (b) Si etched for 1 min at 75k Mag

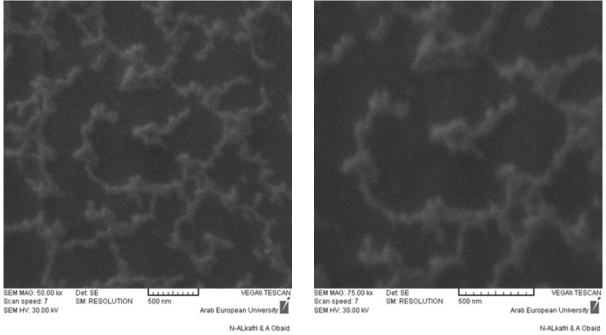

(c) Si etched for 5 min at 50 k Mag (d) Si etched for 5 min at 75 k Mag

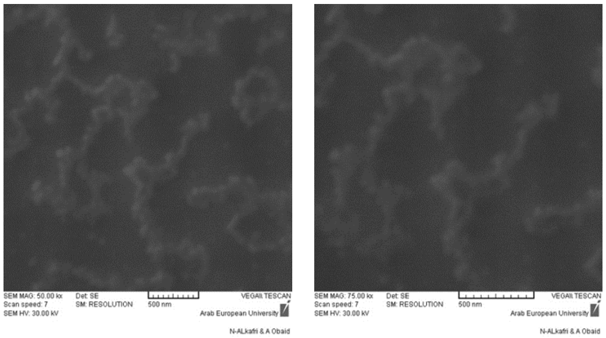

(e) Si etched for 10 min at 50 k Mag (f) Si etched for 10 min at 75 k Mag

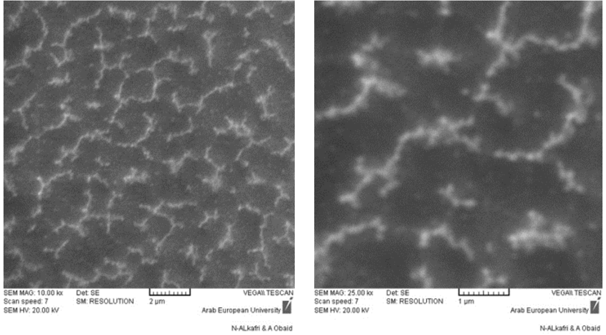

(g) Si etched for 15 min at 10 k Mag (h) Si etched for 15 min at 25 k Mag

Fig. 1. SEM images for the surface of etched Si(100): for 1 min time (a) at 50 k and (b) and 75 k mag, for 5 min (c) at 50 k and (d) 75k mag. for 10 min (e) at 50 k and (f) 75 k mag, and for 15 min (g) at 10 k and (h) 25 k mag.

The silicon became more porous with increase of etching time (for 10 min etching time) and as a consequence the robin became bigger and higher as shown in Figures (1-e) and (1-f) where the SEM images of top view of the surface at 50 k and 75 k magnification, respectively. Similarly, there are higher and longer robin whose length varied form 1 µm to 4 µm for etched Si(100) for 15 min, the Figures (1-g) and (1-h) show SEM top view images at 10 k and 25 k magnifications, respectively. This change of morphology is due to increase of the roughness and therefore we distinguish appearance of nanostructures in the bottom of the cavity, which was observed in our recent work where we used RF sputtering for depositing ZnO films on etched Si(100) [33]. The morphology has an influence on diverse characteristics such as optical ZnS:Cu,Cl [35] and electrical properties [36].

Figure (2-a and b) show AFM images for the surface of etched Si(100) for 1 min etching time (2D and 3D, respectively). These images (2D and 3D) confirm the growth of nanocrystalline structures with spherical forms as shown in the Figure (2-a), where the films are still uniform in morphology. This result is consistent with our previous work [2] where we used RF sputtering and Si(100) substrate non (polished Si). Similarly, Figures (2-c and d) show AFM images 2D and 3D for the sur face Si etching for 5 min time. These images (2D and 3D) show corrugated/ rough (fine porous) structure due to the plasma etching on Si (100).

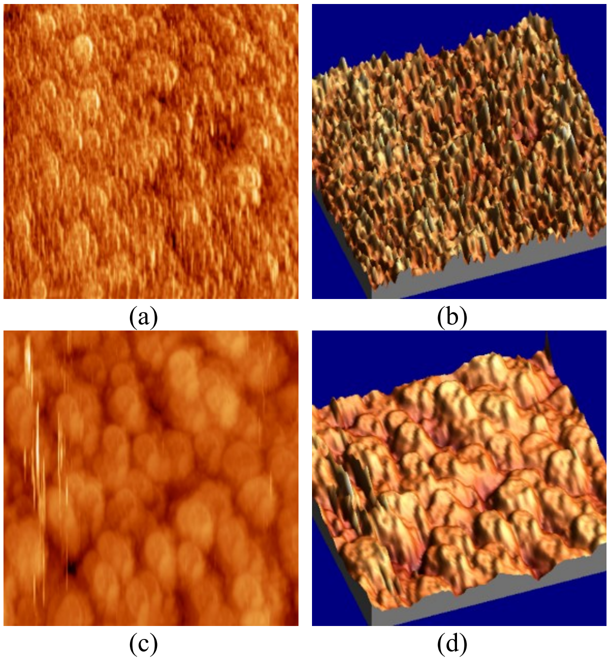
(a) (b)
(c) (d)

Fig. 2. AFM images for the surface of etched Si(100): ,for 1 min time (a) 2D and (b) 3D for 5 min time (c) 2D and (d) 3D at 5x5µm.

Figures (3a and 3-b) and Figures (3c and 3-d) showed the AFM image for 10 min and 15 min etching times at 2D and 3D respectively. The Si substrate has the entire surface in valleys (cavities) and peaks (boundaries).

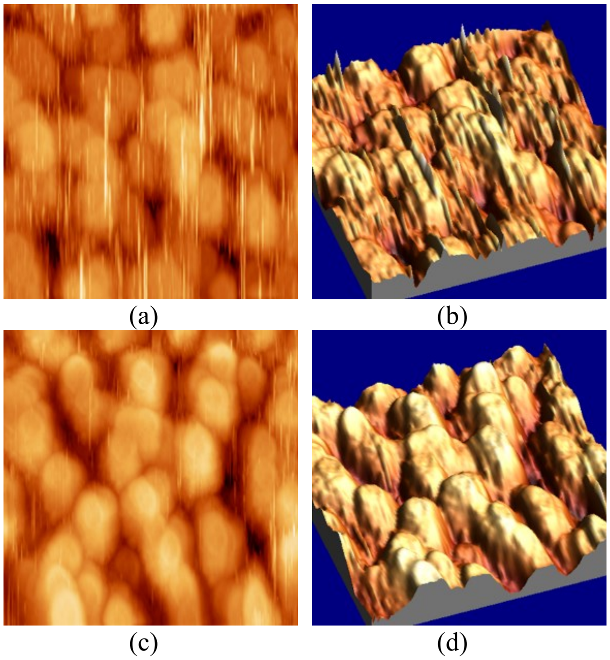
(a) (b)
(c) (d)

Fig. 3. AFM images for the surface of etched Si(100): for 10 min time (a) and (b) 2D and 3D. AFM for 15 min time (c) and (d) (a) and (b) 2D and 3D at 5x5µm .

This appearance has been explained in previous work [23], where Ar/SF6 dry plasma etched silicon substrates (100) are used in other conditions.

SEM STUDY OF ZNO FILMS

SEM SURFACE STUDY OF ZnO FILMS DEPOSITED ON ETCHED Si(100)

Figure (4) shows SEM images of ZnO surface film deposited on etched Si(100) for 1 min time, where (4-a) and (4-b) at 50 k and 75 k magnifications, respectively. The silicon becomes porous and slightly rough but stays nearly dense, due to plasma SF_6 etched dry of PECVD. However, the ZnO film on non-etched Si was very smooth and it is difficult to observe clearly by our SEM, its roughness was very small and less than 1 nm in next paragraph. Similarly, Figures (4-c) and (4-d) show top view SEM images ZnO/Si(100) etched for 5 min at 25 k and 50 k magnifications, respectively. The ZnO film appeared more and more porous and the roughness increased considerably as films developed the robin form (or wires), this result becomes in a good agreement with previous work where we used Ar+SF6 plasma to etch the Si(100).

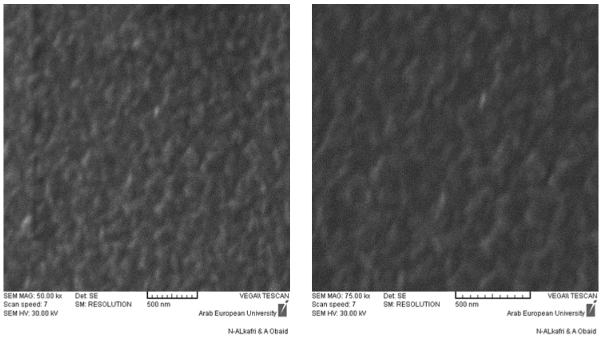

(a) at 50 k mag (b) at 75 k mag

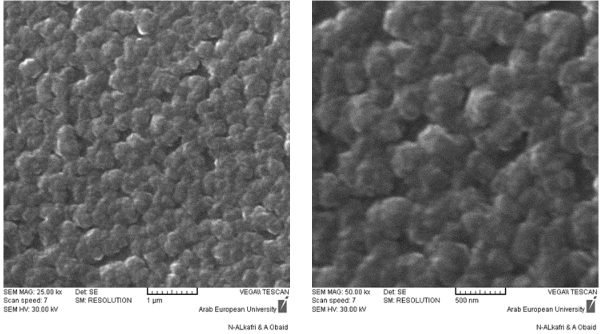

(c) at 25 k mag (d) at 50 k mag

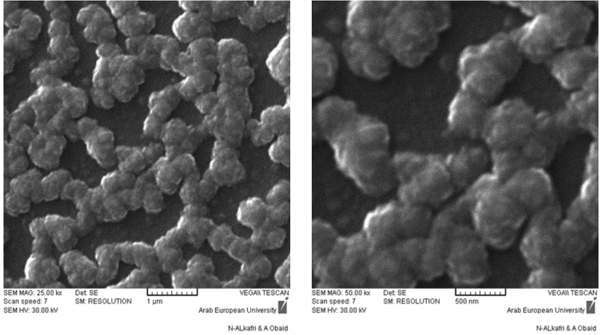

(e) at 25 k mag (f) at 50 k mag

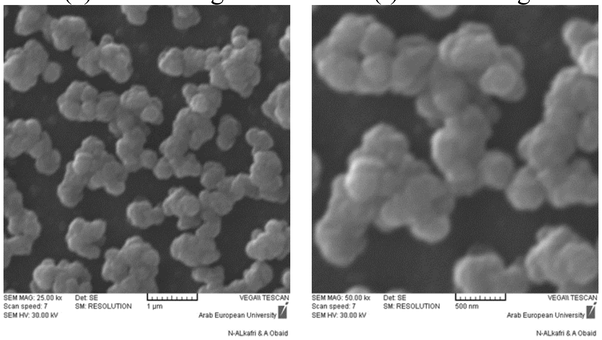

(g) 25 k mag (h) 50 k mag

Fig. 4. SEM images for the surface of ZnO film deposited on etched Si(100): for 1 min time (a) at 75 k and (b) 50 k mag, for 5 min (c) at 25 k and (d) 50 k mag, for 10 min (e) at 25 k and (f) 50 k mag, and for 15 min (g) at 25 k and (h) 50 k mag.

The ZnO film became more porous with increasing the etched time (for 10 min etching time) and as consequence the robin became longer (more black zone indicates to bottom) and higher (their diameter of aggregate or wires varied from 500 nm to 1µm) as shown in Figures (4-e) and (4-f) where the SEM images for top surface at 25 k and 50 k magnification, respectively. Similarly, there are higher and longer robins whose length varied form 1 µm to 4 µm for ZnO film deposited on etched Si(100) for 15 min, as shown in the Figures (4-g) and (4-h) corresponding to top view SEM images at 25 k and 50 k magnifications, respectively.

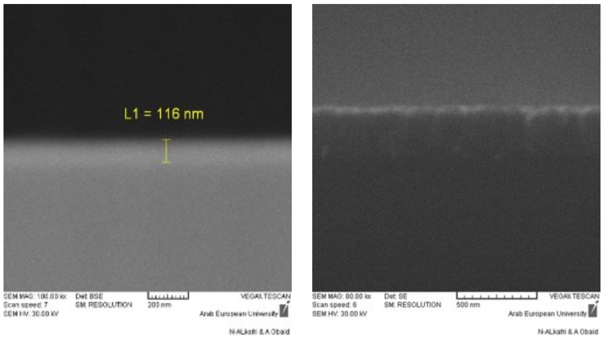

(a) ZnO film on Non-etched substrate at 300k mag (b) ZnO film on etched for 1 min at 80k mag SE

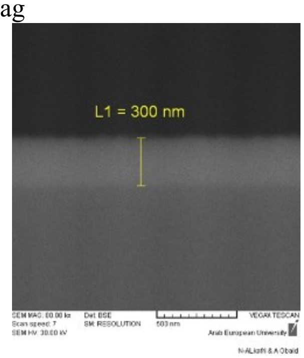

(c) ZnO film on etched for 1 min at 80k mag BSE

Fig. 5. SEM images cross section for ZnO films (a) on non-etched substrate, (b) and (c) for ZnO film on etched for 1 min at 80k mag for SE and BSE respectively.

SEM CROSS SECTION STUDY OF ZnO FILMS

Figure (5-a) shows cross section SEM images of ZnO film deposited on Si non-etched (polished Si). The thickness was about 116 nm and the structure is dense, which is classical growth because the Si is smooth, the film is very smooth due to Ar+ bombardment to the target via magnetron sputtering at optimized conditions (energy and pressure). Figures (5-b) and (5-c) show cross section SEM images of ZnO film deposited on Si etched for 1 min using secondary electron (SE) and backscattering electron (BSE) at 80 k magnifications, respectively.

Figures (6-a) and (6-b) show cross section SEM images of ZnO film deposited on Si etched for 5 min at 75 k magnifications using secondary electron (SE) and backscattering electron (BSE), respectively. Similarly, Figures (6-c) and (6-d) at SE and BSE for ZnO film deposited on etched Si for 10 min at 50 k Magnifications, respectively.

The two ZnO films, deposited on Si etched at 5 min and 10 min, show pores in the film and not dense structure and their thickness is more than the non-etched film (0 min), the thickness was about of 500 nm for etched Si at 5 min and about 700 nm for film deposited on etched Si at 10 min.

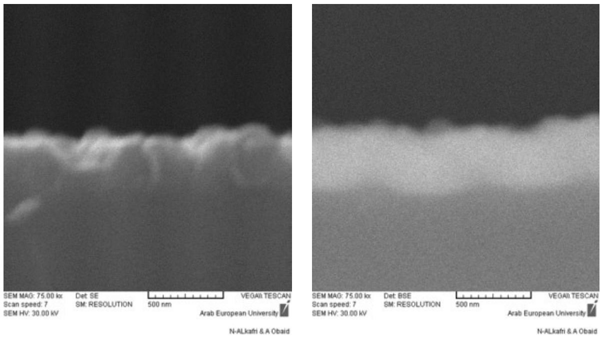

(a) SE etched Si for 5 min at 75k Mag

(b) BSE etched Si for 5 min at 75k Mag

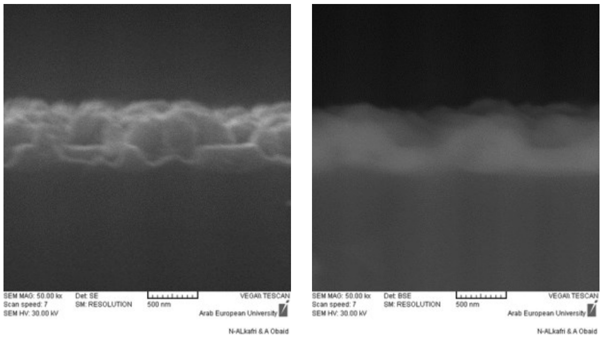

(c) SE etched Si for 10 min at 50k Mag

(e) BSE etched Si for 10 min at 50k Mag

Fig. 6. SEM images cross section for ZnO on etched substrate, (a) and (b) for etched Si for 5 min at 75k using SE and BSE. Images (c) and (d) for etched Si for 10 min at 50 k using SE and BSE respectively.

Figure (7-a) shows cross section SEM images of ZnO film deposited on Si etched for 15 min using secondary electron (SE) at 25 K magnification. Furthermore, Figures (7-b) and (7-c) show the ZnO film on Si etched for 15 min using SE and BSE at magnification 50 K, these images confirm the granular or aggregate structures. We have distinguished two structures, in the interface (bottom in SEM images for top view in last paragraph) the first one is dense and the second is columnar growth and looks like aggregates (or less dense). It is interesting to note that the cavity dimensions, where the diameter was varied from 1 μm to 3 μm with depth was about 250 nm due to etched condition (SF6 plasma).

All the images of Figure (7) confirmed the robin form (which indicate in details in SEM images for the surface of ZnO deposited on etched Si), that justified high roughness morphology for ZnO/Si(100) film with the average thicknesses were about 1000 nm (where 250 nm as dense structure and 750 nm as rough structure).

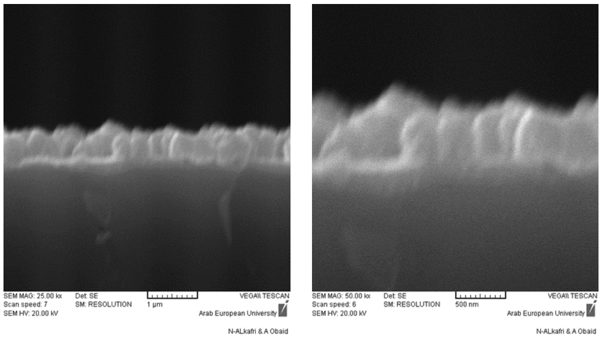

(a) SE at 25 k mag (b) SE at 50 k mag

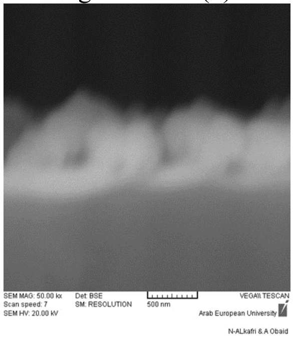

(c) BSE at 50 k mag

Fig. 7. Cross section SEM images of ZnO film deposited on Si etched for 15 min: (a) using SE at 25 K mag, (b) using SE and (c) using backscattering electron at magnification 50 K

Nayef et al[37] present in their results the morphology study showing an improvement in the structural stability of the PS (porous silicon) substrate ('pores' and voids') with crystalline growth of ZnO thin film. This makes porous silicon an adhesive surface for accommodating ZnO into its pores.

AFM STUDY OF ZnO FILM ON ETCHED Si(100)

Figures (8-a and 8-b) show AFM images for ZnO films surface deposited on etched Si(100): for 0 min time (non-etched Si) (a) 5x5µm and (b) 1x1µm. The ZnO film was very smooth, where their roughness is less than 3 nm.

Similarly, AFM images for ZnO deposited on Si etched for 1 min etching time as shown in Figures (8 c-d); where (8-c) and (8-d) correspond to surface area at 5x5µm and 1x1µm, respectively. The ZnO film was smooth and less porous and their roughness less than 5 nm.

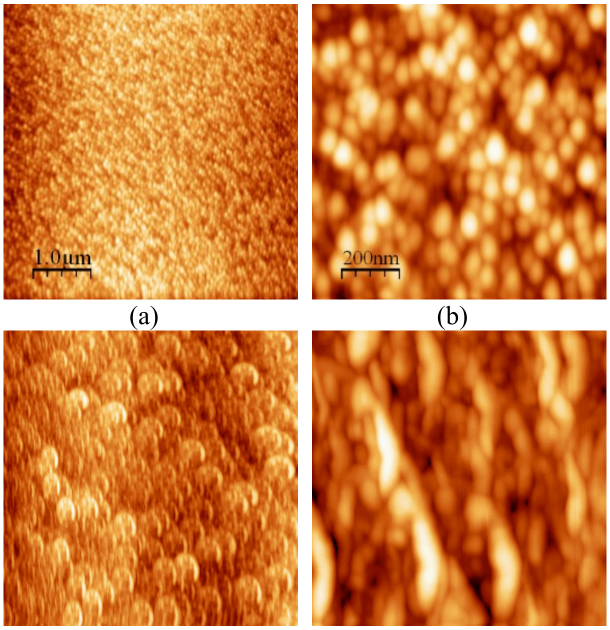

(a) (b)

(c) (d)

Fig. 8. AFM images for ZnO films surface deposited on etched Si(100): for 0 min time (a) 5x5µm and (b) 1x1µm. AFM images for 1 min time ; (c) 5x5µm and (d) 1x1µm.

Figures (9-a and 9-b) show AFM images for ZnO films surface deposited on etched Si(100) for 5 min time (non-etched Si) (a) at 5x5µm and (b) at 1x1µm. The ZnO film was very rough where its roughness is more than 20 nm.

Similarly, Figures (9-c and 9-d) show AFM images for ZnO deposited on Si etched for 10 min time; 5x5µm and 1x1µm area, respectively. The ZnO films porous by their morphology change and their roughness is less than 40 nm at 5x5µm.

Figures (9-e and 9-f) show AFM images for ZnO films on Si etched for 15 min and their is about 81 nm at 5x5µm area, we can see that the morphology of deposited ZnO thin film follows approximately that of substrate (plasma etched Si surface), where the porosity and particle density are rarely changed, while the surface roughness, maximum height, particle and pore sizes were increased as result to deposition and incorporation of ZnO particles into the structure of etched Si(100) surface. The higher values of the achieved porosity *can be explained by* an etching process type, where it was performed in 5% Ar-SF6 plasma which was studied in work of Saloum et al [38].

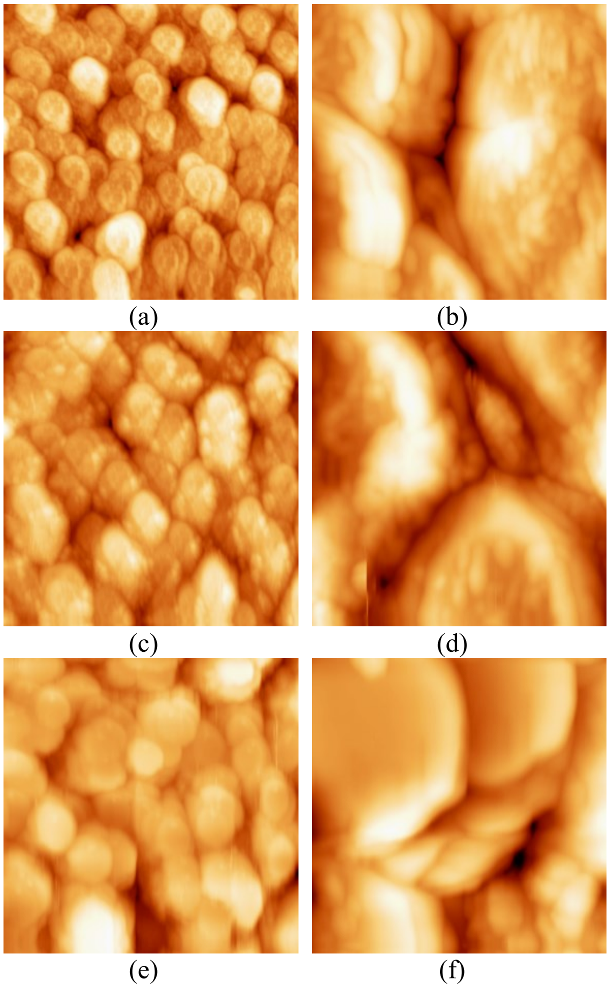
(a) (b)
(c) (d)
(e) (f)

Fig. 9. AFM images for ZnO film; for 5 min time (a) and (b) at 5x5µm and 1x1µm. for 10 min time (c) and (d) at 5x5µm and 1x1µm. for ZnO film on etched Si for 15 min time (e) and (f) at 5x5µm and 1x1µm area.

The Root Mean Square roughness (RMS) at 5x5µm and 1x1µm area as shown in Figure (10) using AFM software, the RMS roughness for ZnO films increased from 2.8 to 19.5 nm at 1x1µm area with increasing the etching time, and it increases from 3.8 nm to 81 nm for ZnO films increasing with increase of etching time at 5x5µm area, this increases of roughness due to increase the etching time and increase the pitting and/or porous in diameters and depth. So the ZnO films follow the same evolution of the substrate, with little difference because the whole surface is covered in valleys (cavities) and peaks (boundaries). There are higher and logger robin whose length varied form 1 µm to 4 µm for ZnO film deposited on etched Si for 10 min and 15 min, as shown in the SEM surfaces figure's top view images.

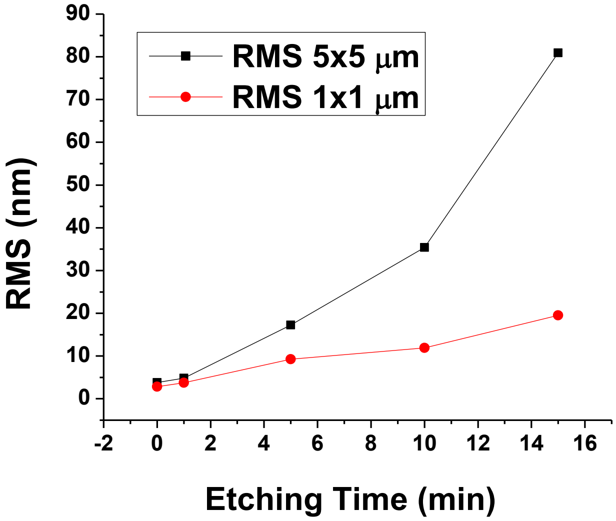

Fig. 10. The roughness (RMS) evolution for ZnO films as a function of etching time for Si at 5x5µm and 1x1µm area.

XPS STUDY OF ZnO FILM

Chemical composition have been investigated for the two ZnO films, as shown in Figure (11), deposited on non-etched Si and etched Si for 15 min substrates. The C_{1s} signal (284.6 eV) was used as a reference signal. XPS curves present peaks correspond to Zn and O elements as main elements, where the C considered as contamination (not desirable and due to the air and/or humidity adsorption).

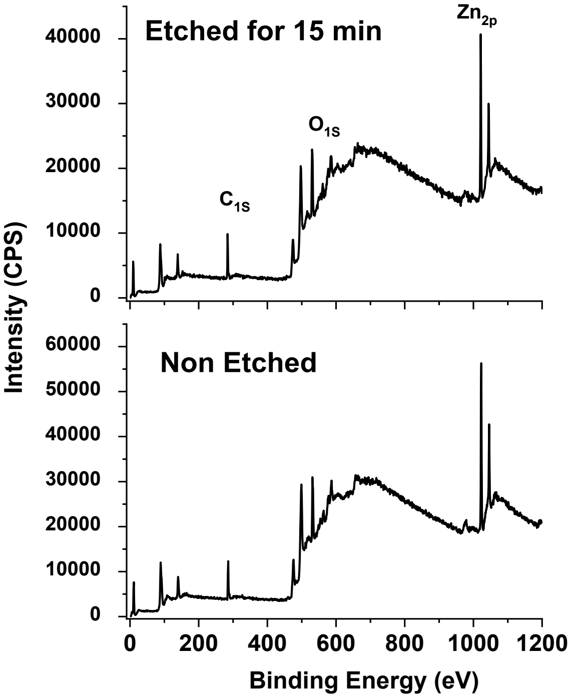

Fig. 11. XPS scans for ZnO thin films deposited on non-etched Si and etched Si for 15 min substrates.

The XPS results of the ZnO film on non-etched Si were essentially composed of O and low percentage of Zn, where the atomic percentages are 87.18 at % and 12.8 at %, respectively. Similarly, atomic percentages for O are 88 % and for Zn is 11 % for ZnO film deposited on etched Si for 15 min. The small amount of Zn in the two films due to the oxidation and/or adsorption in the surface, where the XPS analysis just a few nanometers in the surface.

XRD STUDY OF ZnO FILMS

The Figure 12 shows XRD pattern for ZnO films deposited on polished Si etched for 0 min (non-etched black color), 5 min (blue color) and 15 min (red color) times. The peak at 34.5° corresponding to (002) preferred orientation of the ZnO hexagonal phase (wurtzite structure) for ZnO film deposited on non-etched substrate. However, ZnO films deposited on etched Si (5 and 15 min) have not preferred orientation (they have polycrystalline structure) where the two peaks (100) and (101) observed at 31.74° and 36.30°, respectively. We found that the etched substrate affects the crystallinity and change the preferred orientation, this change in growth mechanism is interesting for several optoelectronics [39] as well as sensing gas applications [40] [41].

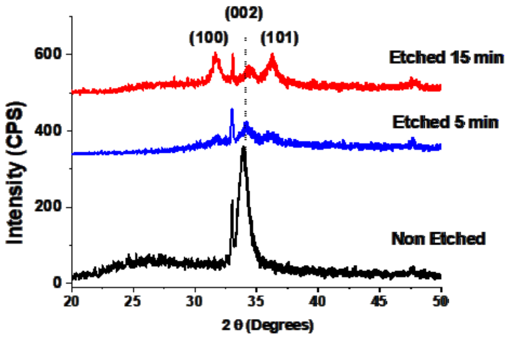

Fig. 12. XRD pattern for ZnO thin films deposited on non-etched Si and etched Si for 5 min and 15 min substrates.

CONTACT ANGLE STUDY OF ZnO FILM

Surface wettability of deposited ZnO films was obtained from WCA measurements. The variation of WCA for the ZnO deposited as a function of etching times was shown in Figure (13). The film deposited on non-etched (0 etching time) shows a hydrophilic surface with WCA of around 96.2°. As the etching time increases, the WCA increases and the surface becomes hydrophobic with WCA of about 134.3°, As the etching time increases for the film deposited Si etched at 15 min. The increase in the WCA refers to decrease in the surface wettability of the deposited film.

Both the surface hydrophobicity and roughness (Figure 10) of the deposited films increase with increasing the etching time of the Si substrate. A good correlation was observed between the SEM micrographs and contact angle results. Also, B. Abdallah et al [34] found the contact angel to increase with the increasing the N_2 partial pressure where, they deposited TiN/ZrN thin films deposited by vacuum arc discharge. Subedi et al [42] investigated the hydrophobic to hydrophilic properties ZnO films via contact angles technique for the effect of aluminum doping on the hydrophilicity of the ZnO film, they found that the nature of the film change from hydrophobic to hydrophilic after the treatment in low pressure DC glow discharge plasma.

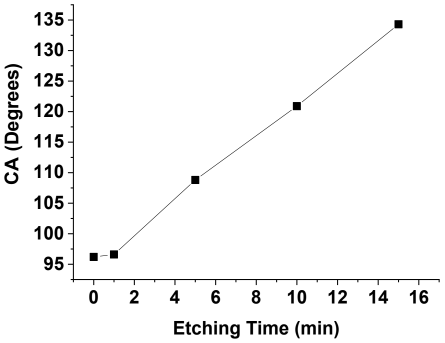

Fig. 13. Variation of water contact angle (WCA) for the ZnO films deposited on etched Si at different time.

CONCLUSION

In this work, three ZnO films were deposited on silicon substrates Si(100) etched at different times and non-etched, the substrate on etched by dry plasma (form 1 min to 15 min) etching time and compared with non-etched substrates (Si(100)). The comparison was systematically achieved to explore the modification on the morphology as well as on the composition for ZnO film deposited on etched substrate and polished substrate (0 min etching time) using SEM cross-section and surface view. Cross-section SEM images show that the ZnO film on Si that is not etched (0 min etching time) was thin (their thickness was about 560 nm), while the ZnO film deposited on etched Si has thick and porous with their thickness varied form 500 nm to 1000 nm with increasing the etching time form 1 min to 15 min. With increasing etching time for Si substrate, the roughness morphology is increase. The percentage of elements is studied by XPS analysis of ZnO films (the un-etched and etched) at 15 min. In addition, water contact angle (hydrophobicity) increases with increasing the roughness and etching time for the ZnO films. XRD characterizations for ZnO films have been studied and related the modification of quality crystallin of ZnO film with Si etching time. The optical (band gap and intensity) measurements will be investigated in our future work to verify the viability of the prepared films for gas sensors and/or optoelectronic applications.

ACKNOWLEDGMENTS

The authors greatly acknowledge funds to this project by Prof I. Othman, the Director General of the Atomic Energy Commission of Syria, Dr S. Saloum for his valuable discussions.

Conflicts of Interest: The authors declare no conflict of interest.

REFERENCE

[1]. Sharma D.K., Shukla S., Sharma K.K., Kumar V. (2022) "A review on zno: Fundamental properties and applications" Materials Today: Proceedings 49: 3028-3035

[2]. Jazmati A.K., Abdallah B., Lahlah F., Abou Shaker S. (2019) "Photoluminescence and optical response of zno films deposited on silicon and glass substrates" Materials Research Express 6(8): 086401

[3]. Abdallah B., Duquenne C., Besland M.P., Gautron E., Jouan P.Y., Tessier P.Y., . . . Djouadi M.A. (2008) "Thickness and substrate effects on aln thin film growth at room temperature" Eur. Phys. J. Appl. Phys. 43(3): 309-313

[4]. VISHNOI S., KUMAR R., SINGH B.P. (2014) "Effect of substrate on physical properties of pulse laser deposited zno thin films" JOURNAL OF INTENSE PULSED LASERS AND APPLICATIONS IN ADVANCED PHYSICS 4(1): 35 - 39

[5]. Yang J., Bahrami A., Ding X., Lehmann S., Kruse N., He S., . . . Nielsch K. (2022) "Characteristics of ald-zno thin film transistor using h2o and h2o2 as oxygen sources (adv. Mater. Interfaces 15/2022)" Advanced Materials Interfaces 9(15): 2270082

[6]. Abdallah B., Hussein R., Al-Kafri N., Zetoun W. (2019) "Pbs thin films prepared by chemical bath deposition: Effects of concentration on the morphology, structure and optical properties" Iranian Journal of Science and Technology, Transactions A: Science 43(3): 1371-1380

[7]. Alnama K., Abdallah B., Kanaan S. (2017) "Deposition of zns thin film by ultrasonic spray

pyrolysis: Effect of thickness on the crystallographic and electrical properties" Composite Interfaces 24(5): 499-513

[8]. Jazmati A.K., Abdallah B. (2018) "Optical and structural study of zno thin films deposited by rf magnetron sputtering at different thicknesses: A comparison with single crystal" Materials Research

[9]. Rahmane S., Abdallah B., Soussou A., Gautron E., Jouan P.-Y., Le Brizoual L., . . . Djouadi M.A. (2010) "Epitaxial growth of zno thin films on aln substrates deposited at low temperature by magnetron sputtering" physica status solidi (a) 207(7): 1604-1608

[10]. Abdallah B., Jazmati A.K., Refaai R. (2017) "Oxygen effect on structural and optical properties of zno thin films deposited by rf magnetron sputtering" Materials Research 20(3): 607-612

[11]. Al-Khawaja S., Abdallah B., Abou Shaker S., Kakhia M. (2015) "Thickness effect on stress, structural, electrical and sensing properties of (0 0 2) preferentially oriented undoped zno thin films" Composite Interfaces 22(3): 221-231

[12]. Li Z., Gao W. (2004) "Zno thin films with dc and rf reactive sputtering" Materials Letters 58(7): 1363-1370

[13]. Youssef S., Combette P., Podlecki J., Asmar R.A., Foucaran A. (2009) "Structural and optical characterization of zno thin films deposited by reactive rf magnetron sputtering" Crystal Growth & Design 9(2): 1088-1094

[14]. Abdallah B., Al-Khawaja S. (2015) "Optical and electrical characterization of (002) preferentially oriented n-zno/p-si heterostructure" Acta physica polonica 128: 283-288

[15]. Zheng Y., Li M., Wen X., Ho H.-P., Lu H. (2020) "Nanostructured zno/ag film prepared by magnetron sputtering method for fast response of ammonia gas detection" Molecules 25(8): 1899

[16]. Abdallah B., Zidan M.D., Allahham A. (2020) "Syntheses, structural and nonlinear optical characteristics of zno films using z-scan technique" Silicon

[17]. Waszkowska K., Chtouki T., Krupka O., Smokal V., Figà V., Sahraoui B. (2021) "Effect of uv-irradiation and zno nanoparticles on nonlinear optical response of specific photochromic polymers" Nanomaterials 11(2): 492

[18]. Bruno E., Strano V., Mirabella S., Donato N., Leonardi S., Neri G. (2017) "Comparison of the sensing properties of zno nanowalls-based sensors toward low concentrations of co and no2" Chemosensors 5(3): 20

[19]. Chebil W., Fourozi A., Azeza B., Sakly N., Mghaieth R., Lusson A., Saler V. (2015) "Comparison of zno thin films on different substrates obtained by size and shape controlled synthesis of semiconductor nanostructures has attracted considerable attention recent years as their physical and chemical properties depend strongly on morphology, size, and dimensions " Indian journal of pure and applied physics 53: 521-529

[20]. Rahmane S., Abdallah B., Soussou A., Gautron E., Jouan P.Y., Le Brizoual L., . . . Djouadi M.A. (2010) "Epitaxial growth of zno thin films on aln substrates deposited at low temperature by magnetron sputtering" physica status solidi (a) 207(7): 1604-1608

[21]. Saloum S., Akel M., Alkhaled B. (2009) "Diagnostic and processing in sf 6 rf remote plasma for silicon etching" Journal of Physics D: Applied Physics 42(17): 175206

[22]. Saloum S., Zrir M.A., Alkhaled B., Shaker S.A. (2018) "Silicon nanostructuring using sf6/o2 downstram plasma etching: Morphological, optical and sensing properties" Materials Research 21(5)

[23]. Alyones J., Salameh M., Abdallah B. (2020) "Investigation of pressure effect on structural, mechanical properties and corrosion performance of crn thin films" Silicon 12(10): 2489-2495

[24]. Abdallah B., Jazmati A.K., Kakhia M. (2018) "Physical, optical and sensing properties of sprayed zinc doped tin oxide films" Optik 158: 1113-1122

[25]. Abdallah B., Kakhia M., Abou Shaker S. (2016) "Deposition of na2wo4 films by ultrasonic spray pyrolysis: Effect of thickness on the crystallographic and sensing properties" Composite Interfaces 23(7): 663-674

[26]. Chebil W., Fourozi A., Azeza B., Sakly N., Mghaieth R., Lusson A., Saler V. (2015) "Comparison of zno thin films on different substrates obtained by sol-gel process and deposited by spin-coating technique " Indian journal of pure and applied physics 53: 521-529

[27]. Inamdar S.I., Rajpure K.Y. (2014) "High-performance metal–semiconductor–metal uv photodetector based on spray deposited zno thin films" Journal of Alloys and Compounds 595: 55-59

[28]. Sánchez G., Abdallah B., Tristant P., Dublanche-Tixier C., Djouadi M.A., Besland M.P., . . . Bologna Alles A. (2009) "Microstructure and mechanical properties of aln films obtained by plasma enhanced chemical vapor deposition" Journal of Materials Science 44(22): 6125-6134

[29]. Vishwakarma R. (2015) "Effect of substrate temperature on zns films prepared by thermal

evaporation technique" Journal of Theoretical and Applied Physics 9(3): 185-192

[30]. Jeyachitra R., Senthilnathan V., Kathirvel D. (2014) "Optical, photoluminescence and electrical properties of vacuum evaporated zns thin films" International Journal of ChemTech Research 6(5): 3152-3159

[31]. Saloum S., Zrir M.A., Alkhaled B., Shaker S.A. (2018) "Silicon nanostructuring using sf 6/o 2 downstram plasma etching: Morphological, optical and sensing properties" Materials Research 21

[32]. Abdallah B. (2020) "Hrtem, xps and xrd characterization of zns/pbs nanorods prepared by thermal evaporation technique" Nanosystems Physics Chemistry Mathematics 11: 1-9

[33]. Abdallah B., Jazmati A.K., Nounou F. (2020) "Morphological, structural and photoresponse characterization of zno nanostructure films deposited on plasma etched silicon substrates" Journal of Nanostructures 10(1): 185-197

[34]. Abdallah B., Naddaf M., A-Kharroub M. (2013) "Structural, mechanical, electrical and wetting properties of zrnx films deposited by ar/n2 vacuum arc discharge: Effect of nitrogen partial pressure" Nuclear Instruments and Methods in Physics Research Section B: Beam Interactions with Materials and Atoms 298: 55-60

[35]. Corrado C., Jiang Y., Oba F., Kozina M., Bridges F., Zhang J.Z. (2009) "Synthesis, structural, and optical properties of stable zns:Cu,cl nanocrystals†" J. Phys. Chem. A 113: 3830-3839

[36]. Erdogan N.H., Kutlu T., Sedefoglu N., Kavak H. (2021) "Effect of na doping on microstructures, optical and electrical properties of zno thin films grown by sol-gel method" Journal of Alloys and Compounds 881: 160554

[37]. Nayef U.M., Muayad M.W., Khalaf H.A. (2014) "Effect of zno layers on porous silicon properties" Int. J. Electrochem. Sci. 9: 2278 - 2284

[38]. Saloum S., Akel M., Alkhaled B. (2009) "Diagnostic and processing in sf6rf remote plasma for silicon etching" Journal of Physics D: Applied Physics 42(17): 175206

[39]. Sharma S., Vyas S., Periasamy C., Chakrabarti P. (2014) "Structural and optical characterization of zno thin films for optoelectronic device applications by rf sputtering technique" Superlattices and Microstructures 75: 378-389

[40]. Muchuweni E., Sathiaraj T.S., Nyakotyo H. (2017) "Synthesis and characterization of zinc oxide thin films for optoelectronic applications" Heliyon 3(4)

[41]. Park S.-H., Lee Y. (2004) "Controlling preferred orientation of zno thin films by atomic layer deposition" Journal of Materials Science 39: 2195-2197

[42]. Subedi D.P., Madhup D.K., Sharma A., Joshi U.M., Huczko A. (2012) "Retracted: Study of the wettability of zno nanofilms" International Nano Letters 2(1): 1